Available online at www.sciencedirect.com
ScienceDirect
Journal of Non-Crystalline Solids 354 (2008) 1703–1714
JOURNAL OF NON-CRYSTALLINE SOLIDS
www.elsevier.com/locate/jnoncrysol

The structure of aluminophosphate glasses revisited: Application of modern solid state NMR strategies to determine structural motifs on intermediate length scales

Sebastian Wegner, Leo van Wüllen *, Grégory Tricot

Institut für Physikalische Chemie, Westfälische Wilhelms-Universität Münster, Correnstrasse 30-36, 48149 Münster, Germany

Received 7 March 2007; received in revised form 21 August 2007

Abstract

In this paper we report a reinvestigation of the network organization in aluminophosphate glasses. Samples were prepared along the $50K_2O$–xAl_2O_3–$(50-x)P_2O_5$ composition line with $0 < x < 20\%$. The evolution of the glass structure upon alumina incorporation into the phosphate network is monitored employing a combination of advanced solid state NMR strategies including $^{31}P\{^{27}Al\}$-CP-HETCOR NMR, $^{31}P\{^{27}Al\}$-REAPDOR NMR, $^{27}Al\{^{31}P\}$-REDOR NMR and 2D ^{31}P-J-RESolved NMR spectroscopy. Details of the employed NMR protocol are given elsewhere. The network organization on intermediate length scales as a function of the alumina content is then described employing a modified Q notation, Q^n_{m,AlO_x}, where n denotes the number of connected tetrahedral phosphate, m gives the number of aluminate species connected to a central phosphate unit and x specifies the nature of the bonded aluminate species (i.e., AlO_4-, AlO_5- or AlO_6-species).

PACS: 61.18.Fs; 61.43.Fs; 61.66.Fn

Keywords: Nuclear magnetic (and quadrupole) resonance; Phosphates; NMR, MAS-NMR and NQR; Medium-range order; Short-range order

1. Introduction

Phosphate based glasses are involved in a wide variety of technological applications including biomaterials [1], sealing glasses [2], anti-oxidation coatings or as confining matrices for nuclear waste material [3], all of which benefit from the low glass transition temperature (T_g) values or from the high thermal expansion coefficient of the phosphate network. However, pure phosphate glasses suffer from a poor chemical durability which severely impedes their straightforward application. The addition of co-oxides, e.g. Al_2O_3 or B_2O_3, has been shown to considerably increase the chemical durability of the phosphate based glasses [4,5], especially improving the resistance against moisture attack. The incorporation of alumina to the phosphate glasses is supposed to induce some cross-linking between the phosphate chains via the formation of Al–O–P linkages, hence increasing the stiffness of the glass network. Although a large number of papers has been devoted to the structural characterization of aluminophosphate glasses [6–11] a concise structural model is still lacking. In the majority of the published data, solid state Nuclear Magnetic Resonance (NMR) spectroscopy has been utilized as the analytical tool. Employing ^{27}Al-(MQ)MAS NMR spectroscopy a quantitative site speciation of the different aluminate species present in the glass system, i.e., aluminium in tetrahedral, pentahedral or octahedral (AlO_4, AlO_5 or AlO_6) coordination becomes possible. The poor resolution of the ^{31}P-MAS

* Corresponding author. Tel.: +49 251 8323445; fax: +49 251 8329159.
E-mail address: wullen@uni-muenster.de (L. van Wüllen).

0022-3093/$ - see front matter © 2007 Elsevier B.V. All rights reserved.
doi:10.1016/j.jnoncrysol.2007.10.034

NMR spectra, which are often characterized by broad and overlapping signals, can be drastically improved when resorting to CP-HETCOR [12,13] spectroscopy, as shown by Egan et al. [8]. In a recent paper [11] we employed a set of advanced solid state NMR strategies to study the network organization in aluminophosphate glasses on intermediate length scales. Employing 2D homo- and heteronuclear correlation techniques, a complete and unambiguous phosphate speciation could be accomplished for a model aluminophosphate glass of composition $50K_2O–10Al_2O_3–40P_2O_5$. $^{31}P\{^{27}Al\}$-CP-HETCOR and $^{31}P\{^{27}Al\}$-HMQC NMR experiments were employed to construct a complete correlation map. These techniques allow the distinction between different phosphate sites via the coordination state of the connected aluminium. The number of phosphate moieties connected to octa-, penta- or tetrahedral aluminium can then be deduced from the 2D spectra. In addition, $^{31}P\{^{27}Al\}$-REAPDOR (Rotational Echo Adiabatic Passage Double Resonance) NMR [14] spectroscopy provides the number of aluminate polyhedra connected to each phosphate species. Finally, J-RESolved NMR experiments [15,16] allow for the determination of the number of phosphate tetrahedra connected to each phosphate species. The combined results then lead to a complete description of the network organization of the investigated glass structure using a Q^n_{m,AlO_x} notation where n denotes the number of connected phosphate, m indicates the number of connected aluminate polyhedra and x identifies the coordination state of the connected aluminium. In addition, the chemical environment of the individual aluminate species can be characterized employing $^{27}Al\{^{31}P\}$-REDOR (Rotational Echo Double Resoance) NMR [17].

In the current paper, this NMR protocol is utilized for an extended in depth study of the effect of aluminium incorporation into the phosphate network in potassium metaphosphate glasses of general composition $50K_2O–xAl_2O_3–(50-x)P_2O_5$, in which the alumina content was varied in the range ($2.5 \leqslant x \leqslant 20$). The results enable us to discuss the changes in the network organization of phosphate glasses upon addition of alumina in considerable detail, indicating different structural motifs on intermediate length scales for alumina-poor and alumina-rich glasses.

2. Experimental procedures

2.1. Synthesis

$50K_2O–xAl_2O_3–(50-x)P_2O_5$ glasses were prepared employing the standard melt quenching technique. Mixtures of appropriate amounts of reagent grade K_2CO_3, $Al(OH)_3$ and $(NH_4)_2HPO_4$ (to obtain 10 g of glass) were heated slowly to 600 °C (1°/min) in an electric furnace to remove H_2O, NH_3 and CO_2. The batch was then directly melted in a Pt crucible during 20 min, before being quenched between two copper plates to obtain colorless and transparent glasses. The melting temperature (in the range of 900–1300 °C) was optimized for each composition to avoid P_2O_5 volatilization. As weight losses ($\Delta m/m$) proved to be less than 3% in all cases, the compositions given are batch compositions. Some glasses were also synthesized from a mixture of $K_4P_2O_7$, Al_2O_3 and P_2O_5. These mixtures were prepared in a glove box to avoid any reaction with moisture and then directly heated at the melting temperature in a covered Pt crucible. The glass transition temperatures were measured with a differential scanning calorimeter at a heating rate of 10 °C/min with an estimated error of ±10 ° C. In Table 1, a compilation of the synthesis parameters and T_g values can be found.

2.2. Solid state NMR

All the different NMR measurements were recorded on a Bruker DSX 400 NMR spectrometer operating at 9.4 T employing a 4-mm triple resonance probe with resonance frequencies of 104.2 MHz and 161.9 MHz for ^{27}Al and ^{31}P, respectively. Radio frequency fields (ν_{RF}) were typically set to 100 kHz for ^{31}P and 35 kHz for ^{27}Al with MAS (Magic Angle Spinning) at 15 kHz. For the 2D $^{31}P\{^{27}Al\}$-CP-HETCOR NMR experiments rather weak matching ν_{rf} fields [18] (approx. 8 kHz for ^{31}P and 6.5 kHz for ^{27}Al; optimized for each sample) have to be used to warrant an efficient cross polarization step. In the J-RESolved experiment [15,16] the signal, obtained through a z-filtered spin echo ($\pi/2–t_1/2–\pi–t_1/2$), is modulated by the homonuclear scalar interaction. The resulting 2D spectrum exhibits a multiplet structure resulting from the resolved homonuclear J-coupling in the indirect dimension from which the number of connected phosphate species can be evaluated. $^{31}P\{^{27}Al\}$-REAPDOR NMR [14] and $^{27}Al\{^{31}P\}$-REDOR NMR experiments [17] were employed to study P–O–Al connectivity by an exploration of the Al–P heteronuclear dipolar coupling. In REDOR, the results from a rotor-synchronized spin-echo experiment for the observed (S) nuclei, defining the full echo intensity S_0, are compared to spectra resulting from an experiment in which the heteronuclear dipolar coupling between nuclei S and I has been reintroduced by the action of rotor-synchronized π-pulses (I-channel) in addition to the S-spin spin-echo pulses. The difference of the spectra from the two experiments then only contains contributions from S nuclei experiencing a dipolar coupling to I nuclei. The magnitude of the REDOR effect depends on the strength of the dipolar coupling and the dipolar evolution time, the latter of which can be controlled by the number of rotor cycles and the MAS frequency. In the case of quadrupolar nuclei as the dephasing I nuclei (as is the case with ^{27}Al), REAPDOR, a variation of REDOR, provides a more efficient dephasing through the application of a long I channel pulse (one third of a full rotation period) in the middle of the pulse sequence. For an analysis of the resulting REAPDOR and REDOR curves, the simulation package SIMPSON was used [19], employing internuclear distances (from crystalline model compounds) as input parameters to evaluate the number of aluminate species connected to a given

Table 1
Synthesis parameters for the KAlP_x glasses

Sample	K_2O (mol%)	Al_2O_3 (mol%)	P_2O_5 (mol%)	T_m	t_m	$\Delta m/m$	T_g
KAlP_2.5	50	2.5	47.5	900	15	2.5	278
KAlP_5	50	5	45	1000	15	3.0	303
KAlP_7.5	50	7.5	42.5	1000	15	0.8	331
KAlP_10	50	10	40	1000	20	2.1	349
KAlP_12.5	50	12.5	37.5	1050	20	2.0	350
KAlP_15	50	15	35	1100	25	1.2	349
KAlP_17.5	50	17.5	32.5	1150	20	0.8	nm
KAlP_20	50	20	30	1300	25	1.2	310

The error on the T_g values is estimated to ±10 °C. The melting (T_m) and glass transition (T_g) temperatures are given in °C; melting time (t_m) is given in minutes and the weight loss ($\Delta m/m$) in %.

phosphorous site with $^{31}P\{^{27}Al\}$-REAPDOR NMR and the number of phosphate species connected to a central aluminate species with $^{27}Al\{^{31}P\}$-REDOR NMR spectroscopy. For further details of the individual NMR experiments, the reader is referred to [11].

3. Results

3.1. Thermal analysis

The evolution of the glass transition temperature with increasing Al_2O_3 content is reported in Fig. 1. Addition of Al_2O_3 first induces an almost linear increase in T_g, reaching a plateau at 350 °C for 10% Al_2O_3. For the extreme Al_2O_3 rich glass sample KAlP_20, a decrease in T_g is observed. The observed behavior for potassium aluminophosphate glasses mirrors that of sodium aluminophosphate glasses [8,21] and other mixed phosphate glass networks (e.g. vanadophosphate glasses [22]). The increase in T_g for moderate alumina content has been ascribed to a cross-linking of the phosphate chains involving AlO_6 bridges.

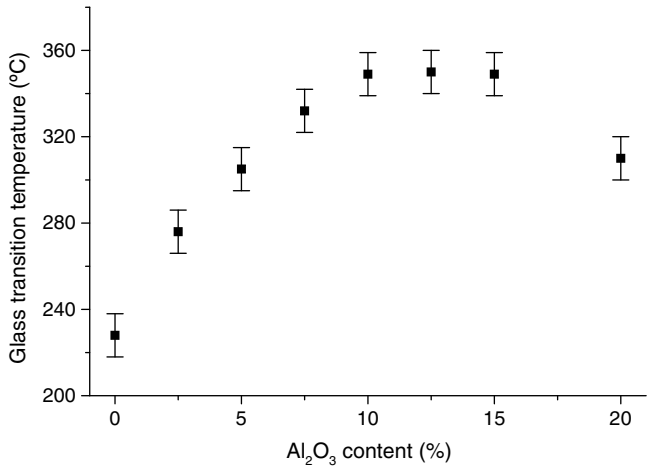

Fig. 1. Glass transition temperatures of the KAlP_x glasses as a function of Al_2O_3 content. The value for the pure metaphosphate glass was taken from Ref. [20].

3.2. ^{27}Al-(MQ)MAS and ^{31}P-MAS NMR

The ^{27}Al-MAS and ^{31}P-MAS NMR spectra are compiled in Fig. 2. From the ^{27}Al-MAS NMR experiments (Fig. 2(a)) the presence of all three coordination states of aluminium which can be found in a glass matrix can be inferred: AlO_6 (−18 ppm), AlO_5 (10 ppm) and AlO_4 (45 ppm). For low Al_2O_3 content, AlO_6 species represent the dominating aluminium environment. Increasing the alumina content of the glass samples leads to a reduction in the amount of six-coordinated aluminium, accompanied by an increase in the fraction of tetrahedrally coordinated aluminium, which constitutes the dominating species at high alumina content. This trend is in good agreement with previous studies of the aluminium speciation in aluminophosphate glasses [6–10]. At low Al_2O_3 content the phosphate network is mainly formed by Q^1-species and charge balancing of the aluminophosphate network favors the AlO_6 coordination (as in the $KAlP_2O_7$ structure [23]); at higher Al_2O_3 content, the phosphate network is mainly constituted by isolated orthophosphate species (Q^0) and

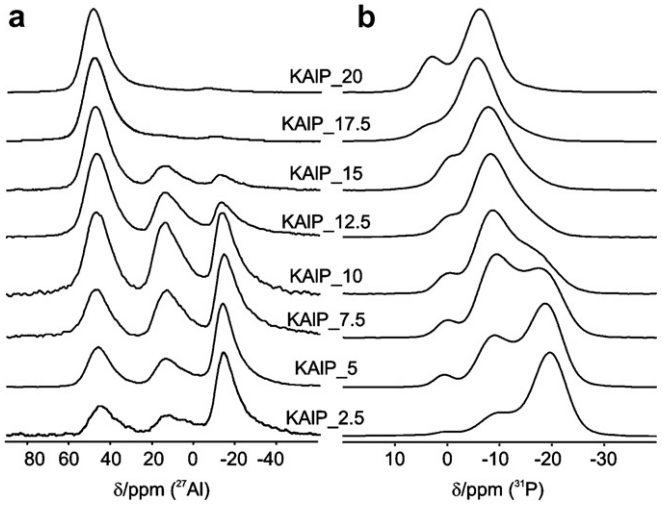

Fig. 2. ^{27}Al-MAS (a) and ^{31}P-MAS NMR spectra (b) for the KAlP_x glasses ($2.5 \leqslant x \leqslant 20$).

charge balance is maintained if aluminium is in tetrahedral coordination (as in the $K_3Al_2(PO_4)_3$ structure [24]). The turnover from a AlO_6 dominated glass structure to a AlO_4 dominated glass structure occurs for the KAlP_10 glass sample which has a O/P ratio of 3.5. The ^{27}Al NMR parameters (δ_{iso}, C_Q, rel. fraction of the individual sites), as determined from the ^{27}Al-MAS NMR or ^{27}Al-MQMAS NMR spectra (not shown) are collected in Table 2.

The ^{31}P-MAS NMR spectra are plotted in Fig. 2(b). At low Al_2O_3 content (KAlP_2.5 and KAlP_5), three different resonances can easily be distinguished around 0 ppm, −10 ppm and −20 ppm. The two signals at 0 ppm and −20 ppm are indicative of the two pure phosphate species Q^1_0 and Q^2_0 as found in binary alkali phosphates [25]. The resonance around −10 ppm then has to be assigned to phosphate species connected to one or more aluminate species. Unfortunately, the poor resolution prevents an unambiguous deconvolution and hence a determination of the number of mixed alumophosphate species and their quantification proves impossible without any further information. The intensity of this signal increases with increasing alumina content up to the KAlP_10 glass composition, supporting the assignment to mixed aluminophosphate species. For the highest Al_2O_3 contents (glasses KAlP_17.5 and KAlP_20), two resonances at 3 and −6 ppm are observed. This limited spectral resolution, especially in the spectra of the glass samples of medium alumina content, impedes a detailed analysis of the structural changes in the phosphate network upon alumina incorporation based on the ^{31}P-MAS NMR spectra alone and we have to resort to heteronuclear correlation techniques (as described in [8,9,11]) to increase the spectral resolution.

3.3. $^{31}P\{^{27}Al\}$-CP-HETCOR NMR

^{31}P{^{27}Al}-CP-HETCOR NMR experiments for glass samples KAlP_5, KAlP_7.5, KAlP_10, KAlP_15 and KAlP_20 are compiled in Fig. 3. The spectra on the right represent slices parallel to the direct dimension (F2) taken at the position of AlO_6 (i), AlO_5 (ii) and AlO_4 (iii). For low alumina contents, the 1D slices taken from the CP-HETCOR spectra are dominated by the signals of five different phosphate units which experience spatial proximity to aluminate species. We find two signals at −7.8 ppm and −16.2 ppm from phosphate groups which are connected to AlO_6 moieties, a signal at −8.2 ppm, accompanied by a shoulder at −15.7 ppm for phosphate species with connection to penta-coordinated aluminium and a single ^{31}P signal, indicative of a phosphate unit with connection to AlO_4 at −11.5 ppm. With increasing amount of alumina up to 10% (KAlP_10 sample) the same sites are resolvable with only minor deviations in chemical shifts (i.e., −7.4 ppm / −15.7 ppm for the phosphate species connected to AlO_6, −8.1 ppm / −15.1 ppm for those with spatial proximity to AlO_5 and −11.1 ppm for the phosphate unit with connection to AlO_4), accompanied by a considerable increase in the relative fraction of the signal at −11.1 ppm. Dramatic changes in the phosphate site speciation, however, can be observed if the alumina content is increased above 10%. The intensity for the two sites connected to AlO_6 and AlO_5 centered around −16 ppm considerably decreases and a new signal at −5.9 ppm in the slices taken at the position of AlO_4 is becoming observable. Upon further increase of the alumina content this signal evolves as the dominant contribution, accompanied by a new signal at +3 ppm for the KAlP_20 glass, again representing phosphate species with spatial proximity to AlO_4 units.

The results of the CP-HETCOR NMR experiments – the separation of the signals for phosphate species bonded to different aluminate polyhedra – can now be employed to accurately identify and quantify the different phosphate species contributing to the overall broad ^{31}P-MAS NMR signal (cf. Fig. 2(b)). The signal positions and line width for the individual signals identified in slices i, ii and iii of the 2D CP-HETCOR NMR spectra were taken as input parameters for a detailed line fitting procedure of the ^{31}P-MAS NMR spectra employing the DMFIT software [26]. The relative proportions of the different phosphate species (including Q^1_0, Q^2_0 and the phosphate species connected to

Table 2
^{27}Al NMR parameters for the KAlP_*x* glasses as obtained from ^{27}Al-MQMAS (samples KAlP_7.5, KAlP_10, KAlP_12.5, KAlP_15) or ^{27}Al-MAS NMR (KAlP_2.5, KAlP_5, KAlP_20)

Sample	AlO_4			AlO_5			AlO_6		
	%	δ_{iso}/ppm	SOQE/MHz	%	δ_{iso}/ppm	SOQE/MHz	%	δ_{iso}/ppm	SOQE/MHz
KAlP_2.5	21[a]	45.7[b]	–	18[a]	14.5[b]	–	61[a]	−13.9[b]	–
KAlP_5	25[a]	46.5[b]	–	21[a]	14.4[b]	–	54[a]	−13.7[b]	–
KAlP_7.5	29	50.8	3.2	21	18.0	3.8	50	−11.2	2.6
KAlP_10	45	49.5	3.4	32	18.4	4.1	23	−10.8	3.2
KAlP_12.5	65	51.2	3.5	19	19.5	3.6	16	−10.1	2.8
KAlP_15	75	50.9	3.7	16	19.1	3.8	9	−9.7	3.3
KAlP_20	95[a]	48.9[b]	–	–	–	–	5[a]	−7.9[b]	–

[a] Relative fractions determined by an integration of the individual ^{27}Al-MAS NMR lines.
[b] Position of peak maximum in ^{27}Al-MAS NMR spectrum.

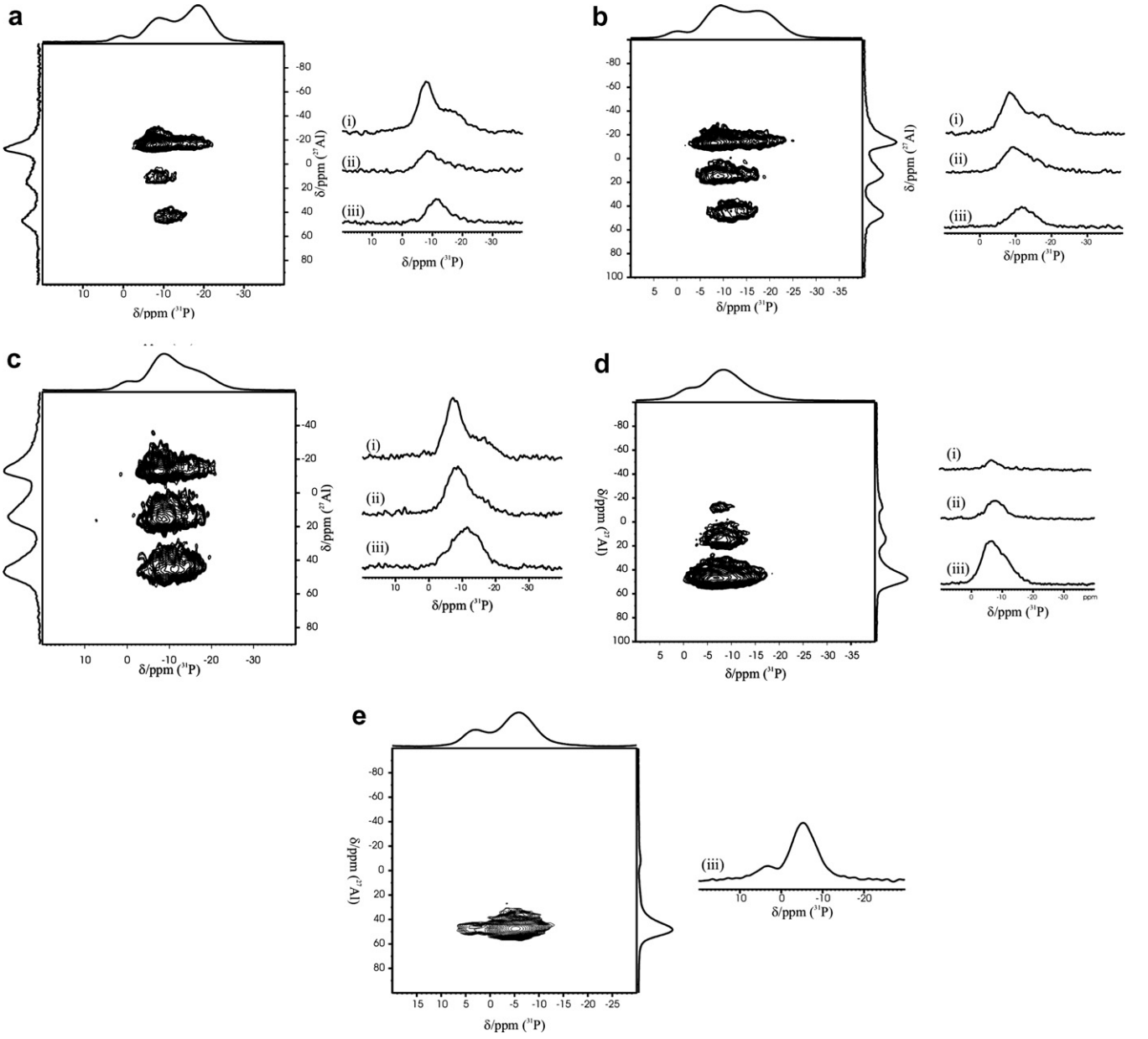

Fig. 3. $^{31}P\{^{27}Al\}$-CP-HETCOR NMR experiments for glass samples KAlP_5 (a), KAlP_7.5 (b), KAlP_10 (c), KAlP_15 (d) and KAlP_20 (e). Spectra on the right of each 2D spectrum represent slices parallel to the direct dimension (F2) taken at the position of AlO_6 (i), AlO_5 (ii) and AlO_4 (iii).

Table 3
Results from a DMFIT [26] analysis of the ^{31}P-MAS NMR spectra of the KAlP_*x* glasses with the line widths and positions as determined from the CP-HETCOR experiments taken as input parameters

KAlP_*x*	Q^n_m,$AlO_{5/6}$	Q^n_m,$AlO_{5/6}$	Q^n_m, AlO_4	Q^n_m, AlO_4	Q^n_m, AlO_4	Q^2_0	Q^1_0
δ/ppm	−8	−16	−12	−6	3	−18	0
2.5	15	11	–	–	–	72	2
5	29	12	10	–	–	44	5
7.5	30	22	15	–	–	27	6
10	30	18	34	–	–	11	7
12.5	33	–	36	9	–	10	12
15	8	–	34	34	2	10	12
17.5	–	–	13	74	8	–	5
20	–	–	–	78	22	–	–

The numbers given represent the relative fraction of the individual lines given in %.

AlO_6-, AlO_5- or AlO_4-moieties) present in the amorphous network were analyzed for each sample and reported in Table 3.

Since the high spectral resolution achieved in the CP-HETCOR spectra does not prevail in the one-dimensional ^{31}P spectra (^{31}P-MAS or $^{31}P\{^{27}Al\}$-REAPDOR NMR, vide infra), the two signals identified at −7.4 ppm and −8.1 ppm and the two signals at −15.4 ppm and −16.2 ppm were treated as a single signal each, since a meaningful deconvolution seems not possible in the 1D spectra.

According to the CP-HETCOR results, at very low alumina content the aluminophosphate network is predominantly constituted by the two pure phosphate species Q^2_0 and Q^1_0 in combination with two phosphate species connected to AlO_6 units and two phosphate species connected to AlO_5 units. At higher alumina content, Q^2_0 and the two sites at −16 ppm connected to AlO_5 and AlO_6 units, respectively, decrease in favor of a new AlO_4 connected phosphate site at −5.9 ppm. With further Al_2O_3 addition, the only aluminium coordination present is AlO_4, connected to two different phosphate species with chemical shifts of 3 ppm and −6 ppm. Having identified the number of the different phosphate moieties present in the glass matrix as well as the coordination state of the connected aluminium (x in the Q^n_{m,AlO_x}), the next step in a detailed

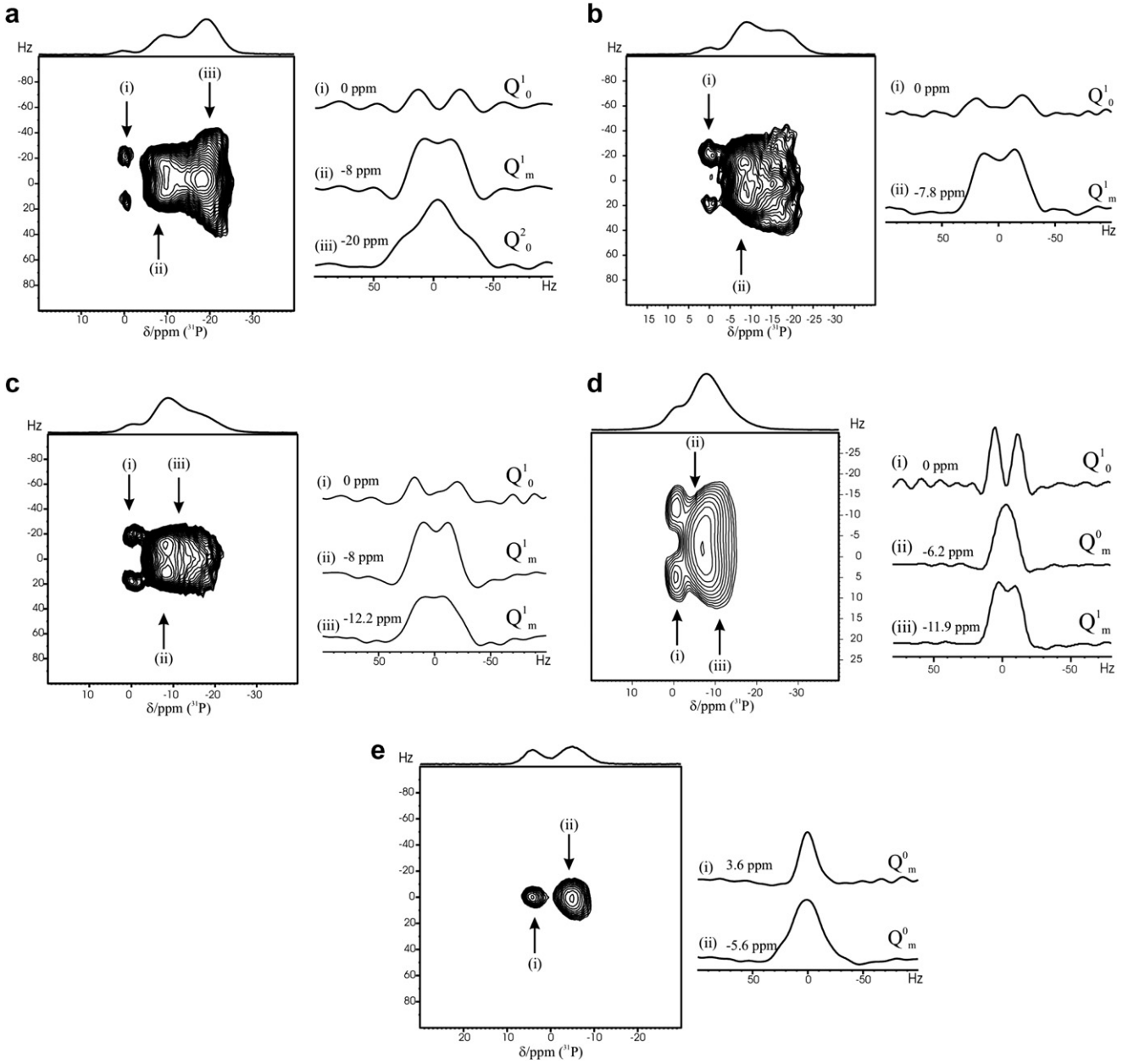

Fig. 4. 2D ^{31}P-J-RESolved NMR spectra for KAlP_5 (a), KAlP_7.5 (b), KAlP_10 (c), KAlP_15 (d) and KAlP_20 (e).The 1D spectra on the right of each 2D spectrum represent slices parallel to the indirect (F1) dimension at the indicated positions giving the multiplet structure.

characterization of the structural motifs on intermediate length scales is the analysis of the number of chemically bonded phosphate and aluminate species (n and m in the Q^n_{m,AlO_x} notation). The values for n can be determined by 2D ^{31}P-JRESolved NMR spectroscopy, m becomes accessible employing $^{31}P\{^{27}Al\}$-REAPDOR NMR spectroscopy, the results for both will be discussed in the next two paragraphs.

3.4. ^{31}P J-RESolved NMR spectroscopy

The ^{31}P J-RESolved technique enables the determination of the condensation degree of the phosphate species present in the glass matrix (n in the Q^n_{m,AlO_x} notation). 2D ^{31}P-J-RESolved NMR spectra for the samples KAlP_5, KAlP_7.5, KAlP_10, KAlP_15 and KAlP_20 are collected in Fig. 4. The one-dimensional spectra on the right of each 2D spectrum represent slices parallel to the F1 axis (indirect dimension) at the indicated positions. From the resolved multiplet structure in these slices we can now determine the condensation degree of the phosphate species in question.

For sample KAlP_5, two resolved doublets for the signals at 0 ppm and −8 ppm, indicative of Q^1 environments (i.e., a phosphate species connected to one further phosphate group) and one triplet for the signal at −20 ppm, characteristic of a Q^2 site, can be identified. Likewise, for samples KAlP_7.5 and KAlP_10, the spectra indicate resolved doublets for the signals at 0 ppm, −8 ppm and −12 ppm, indicating a Q^1 structure for all three sites. Unluckily, for the signals around −16 ppm (connected to AlO_5 or AlO_6 units, vide supra), we were not able to identify any resolved multiplets due to the severe spectral overlap with the triplet signal from the Q^2_0 site at approx. −18 ppm. For the signals observed in the high alumina samples (i.e., the signals at −6 ppm and +3 ppm, both of which exhibit connectivity to tetrahedral aluminate species), singlets can be observed in the JRESolved spectra, indicating Q^0 species.

3.5. $^{31}P\{^{27}Al\}$-REAPDOR NMR experiments

The $^{31}P\{^{27}Al\}$-REAPDOR NMR experiments were performed to determine the number of connected aluminate species to a given phosphorous site, i.e., m in $Q^n_{m,AlOx}$. Results for the REAPDOR experiments for glass samples KAlP_5, KAlP_10 and KAlP_20 are collected in Figs. 5–7. All figures are arranged as follows. The top spectrum (i) on the left side represents the full ^{31}P echo signal S_0, generated by a train of rotor-synchronized ^{31}P-π-pulses. Spectrum (ii) was obtained employing an additional ^{27}Al pulse of length $\tau_r/3$ in the middle of the pulse sequence, leading to a reduced signal intensity for those ^{31}P signals which originate from phosphorous sites with spatial proximity to aluminate species. Spectrum (iii) then gives the difference of the above two experiments and contains only contributions from phosphate species with a spatial proximity to aluminate species. The result of a deconvolution of these spectra employing the DMFIT [26] software is shown in the bottom spectra (iv). The resulting REAPDOR evolution curves for the individual signals for the different glasses, obtained by a variation of the number of rotor cycles, are given in Figs. 5(b), 6(b) and 7(b), in which the symbols represent the experimental data and the solid and dashed lines results from SIMPSON simulations. In these simulations, we assumed a ^{27}Al–^{31}P internuclear distance of 3.1 Å for a P–O–AlO_4 linkage and a distance of 3.2 Å for a P–O–AlO_6 linkage. These values were taken

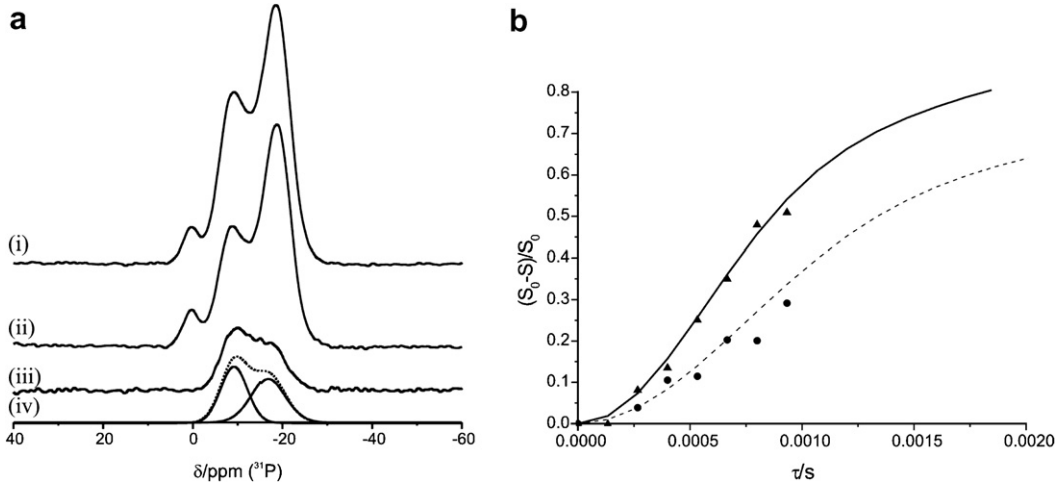

Fig. 5. $^{31}P\{^{27}Al\}$-REAPDOR NMR data for glass KAlP_5. (a) top spectrum (i) represents the full ^{31}P echo signal S_0, spectrum (ii) the $^{31}P\{^{27}Al\}$-REAPDOR NMR spectrum giving the reduced signal intensity S for the individual signals and (iii) gives the difference (i)–(ii). The deconvolution of (iii) into the individual components is shown in (iv), (b) REAPDOR evolution curves for the individual signals together with the results of SIMPSON simulations; full triangles: experimental data for the signal at −16 ppm; full circles: data for the signal at −8 ppm; dashed line: SIMPSON simulation assuming a P–Al two spin interaction with a P–Al distance of 3.2 Å; solid line: SIMPSON simulation assuming a P–Al_2 three spin interaction with P–Al distances of 3.2 Å.

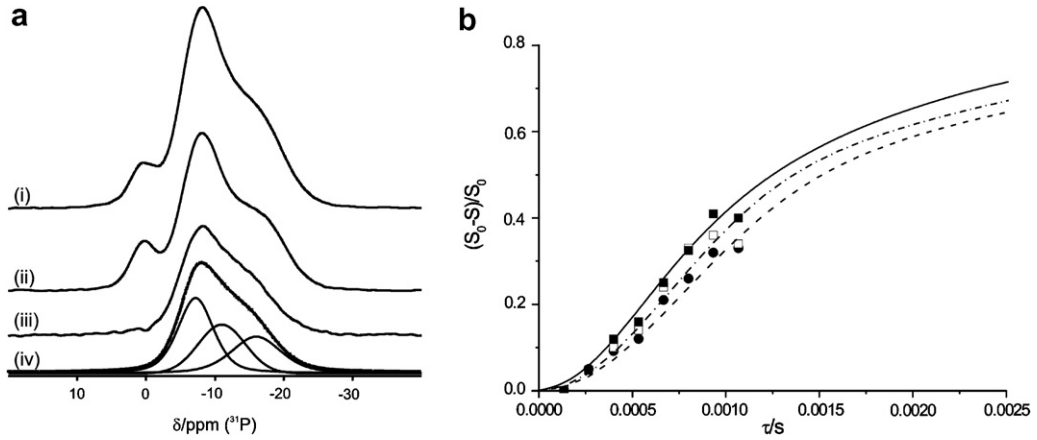

Fig. 6. (a) $^{31}P\{^{27}Al\}$-REAPDOR NMR spectra (16 rotor cycles) for glass KAlP_10. The arrangement of the spectra is the same as in Fig. 5. (b) REAPDOR evolution curves for the individual signals at −8 ppm, −12 ppm and −16 ppm together with the results of SIMPSON simulations; full squares: signal at −16 ppm; open squares: signal at −12 ppm; full circles: signal at −8 ppm; The lines are results of SIMPSON simulations assuming a P–Al distance of 3.2 Å and a P–Al_2 three spin interaction (solid line), a P–Al distance of 3.2 Å and a P–Al two spin interaction (dashed line), and a P–Al distance of 3.1 Å and a P–Al two spin interaction (dash–dotted line).

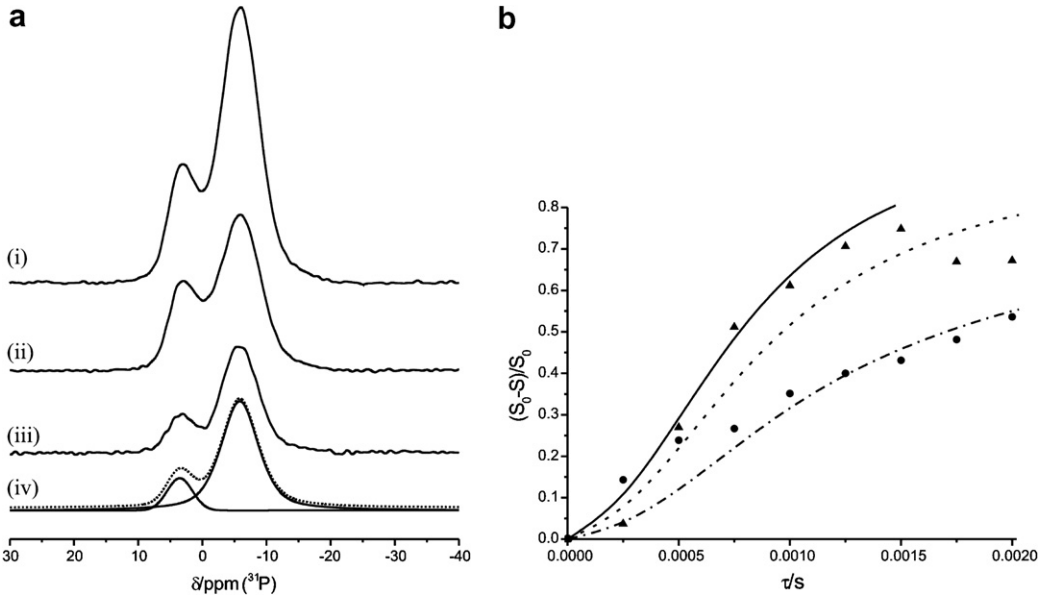

Fig. 7. (a) $^{31}P\{^{27}Al\}$-REAPDOR NMR spectra for glass KAlP_20. The arrangement of the spectra is the same as in Fig. 5. (b) REAPDOR evolution curves for the individual signals at +3 ppm (full circles) and −6 ppm (full triangles) together with SIMPSON simulations assuming a P–Al_3 four spin interaction (solid line), a P–Al three-spin interaction (dashed line) and a P–Al two-spin interaction (dash–dotted line). A P–Al distance of 3.1 Å was used in the simulations.

from crystalline model compounds, i.e., $KAlP_2O_7$ and $K_3Al_2(PO_4)_3$. For glass sample KAlP_5, two different signals at −8 ppm and −16 ppm can be observed in the REAPDOR difference signal. The absence of the signal at 0 ppm in the difference spectrum confirms the assignment of this line to Q_0^1 species. As stated above, a deconvolution of these two lines in two separate lines each (at −7.4 ppm and −8.1 ppm or −15.4 ppm and −16.2 ppm, as found in the CP-HETCOR experiments) proves to be not feasible due to the severe overlap of the signals. The REAPDOR evolution curves obtained for the site at −8 and −16 ppm can now be compared to the results of the SIMPSON simulations. The solid line (Fig. 5(b)) was generated assuming a P–Al_2 three spin system with P–Al distances of 3.2 Å, the dashed line represents results from a simulation assuming a P–Al two spin system (i.e., one ^{27}Al nucleus in a distance of 3.2 Å). Details of the SIMPSON simulations can be found elsewhere [11]. Comparing the experimental data with these simulations, the signal at −16 ppm can safely be assigned to phosphate species connected to two hexa-coordinated aluminate species, (i.e., $m = 2$ in the in Q^n_{m,AlO_x} notation), whereas the signal at −8 ppm has to be designated to phos-

phate species experiencing a heteronuclear dipolar interaction to only one single ^{27}Al nucleus, thus $m = 1$ in the Q^n_{m,AlO_x} notation. The REAPDOR results for glass sample KAlP_10 (cf. Fig. 6) confirm the assignment for the signals at −8 ppm and −16 ppm. In addition, a third component at −11.1 ppm can be identified in the REAPDOR difference spectra (spectrum (iii) in Fig. 6), which originates from phosphate moieties connected to AlO_4 units, as exemplified by the CP-HETCOR results. The SIMPSON simulations for this species are compatible with the assumption of a single P–O–Al connection with a distance of 3.1 Å, i.e., $m = 1$ in the Q^n_{m,AlO_x} notation.

For the two phosphate species responsible for the two signals at +3 ppm and −6 ppm, discernable in the REAPDOR difference spectrum of KAlP_20 (cf. Fig. 7, spectrum (iii)), the SIMPSON simulations indicate the presence of one neighboring tetra-coordinated aluminate species for the phosphate species resonating at 3 ppm ($m = 1$) and three neighboring aluminate tetrahedra for the second phosphate species ($m = 3$).

From the combined results of the experiments presented, a decisive description of the structural motifs on intermediate length scales employing the modified Q notation becomes possible. As an example, for the phosphate species responsible for the signal at −8 ppm, we identify $n = 1$ from the JRESolved NMR experiment, $m = 1$ from the ^{31}P{^{27}Al}-REAPDOR-NMR experiment and $x = 6$ from ^{31}P{^{27}Al}-CP-HETCOR NMR experiments, leading to an assignment as Q^1_{1,AlO_6}. The final assignments for all identified signals are collected in Table 4.

3.6. ^{27}Al {^{31}P}- REDOR NMR experiments

The ^{27}Al{^{31}P}-REDOR NMR experiments were performed to analyze the number of neighboring phosphate polyhedra around a central AlO_x unit. In Figs. 8 and 9 the results for glass samples KAlP_5 and KAlP_12.5 are collected. The arrangement of the spectra mirrors that of the REAPDOR results given before. A pronounced REDOR effect indicating spatial proximity to phosphate polyhedra is observed for all three different AlO_x species present in the glass sample. The REDOR evolution curves are compiled in Figs. 8(b) and 9(b). Full triangles represent AlO_6 units, open squares AlO_5 species and full circles AlO_4 moieties.

The lines are the results from SIMPSON simulations assuming Al–P multiple spin systems (AlP_2 three-spin interaction, AlP_4 five-spin interaction and AlP_6 seven-spin interaction). Although the S/N ratio proves to be somewhat limited, especially for the AlO_4 coordination in the KAlP_5 sample and the AlO_6 coordination in the KAlP_12.5 glass sample, the results indicate a full coordination of the different aluminate species by phosphate species, i.e., AlO_4 is connected to four, AlO_5 to five and AlO_6 to six phosphate polyhedra, thereby fulfilling the Loewenstein rule [27] which prohibits a direct Al–O–Al connectivity for tetrahedrally coordinated aluminate species. A comparison of the experimental REDOR curves with published data on crystalline $Al(PO_3)_3$ ($Al(OP)_6$ structure) and $AlPO_4$ ($Al(OP)_4$ structure) [28] supports the above assignment.

Table 4
Phosphate speciation Q^n_{m,AlO_x} deduced from the NMR experiments

δ_{iso}/ppm	Q^n_m
−18	Q^2_0
0	Q^1_0
−8	Q^1_{1,AlO_6}
−16	Q^1_{2,AlO_6}
−7	Q^1_{1,AlO_5}
−15	Q^1_{2,AlO_5}
−12	Q^1_{1,AlO_4}
−6	Q^0_{3,AlO_4}
3	Q^0_{1,AlO_4}

n (the number of connected phosphate polyhedra) is evaluated from the ^{31}P J-RESolved NMR experiments; m (the number of connected aluminate polyhedra) is determined from the ^{31}P{^{27}Al}-REAPDOR NMR experiments; x (specifying the nature of the connected aluminate species) is taken from the ^{31}P{^{27}Al}-CP-HETCOR NMR spectra.

4. Discussion

The combined results of the ^{31}P{^{27}Al}-CP-HETCOR-, 2D ^{31}P-J-RESolved- and ^{31}P{^{27}Al}-REAPDOR-NMR experiments presented above, accumulating in the assignment Q^n_{m,AlO_x} to the various identified phosphate species and the ^{27}Al{^{31}P}-REDOR NMR results identifying the intermediate range ordering around a central AlO_x species as $Al(OP)_4$, $Al(OP)_5$ and $Al(OP)_6$ now allow for a detailed description of the network organization in aluminophosphate glasses as a function of the alumina content.

Low Al_2O_3 content glasses: A phosphate network built from infinite chains of phosphate tetrahedra connected to two other phosphate polyhedra (Q^2_0, as in a pure metaphosphate glass) marks the starting point for our discussion. Insertion of small amounts of alumina to the glasses leads to a depolymerisation of the phosphate network and thus induces the formation of different Q^1 sites. The two principal phosphate moieties identified by CP-HETCOR and characterized by REAPDOR and J-RESolved spectroscopy are connected to AlO_6 species, which is the main aluminium coordination state at low Al_2O_3 content: one is only connected to a single AlO_6 octahedron (Q^1_{1,AlO_6}), the second one is connected to two AlO_6 units (Q^1_{2,AlO_6}). Other Q^1_1 species connected to penta- and tetrahedral aluminium can also be observed, but their relative fractions are rather low and therefore they will not pose a significant implication for the glass structure. Apart from the Q^2_0, Q^1_{1,AlO_6} and Q^1_{2,AlO_6} sites Q^1_0 species are also present in the glass matrix. ^{31}P-BABA (Back to back) [29] as well as INADEQUATE (Incredible Natural Abundance DoublE QUAntum Transfer Experiment) experiments [30] performed on the KAlP_7.5 glass sample (not shown) indicate that all these Q^1 sites are consumed for the termination of Q^2 chains and not involved in pyrophosphate groups. From

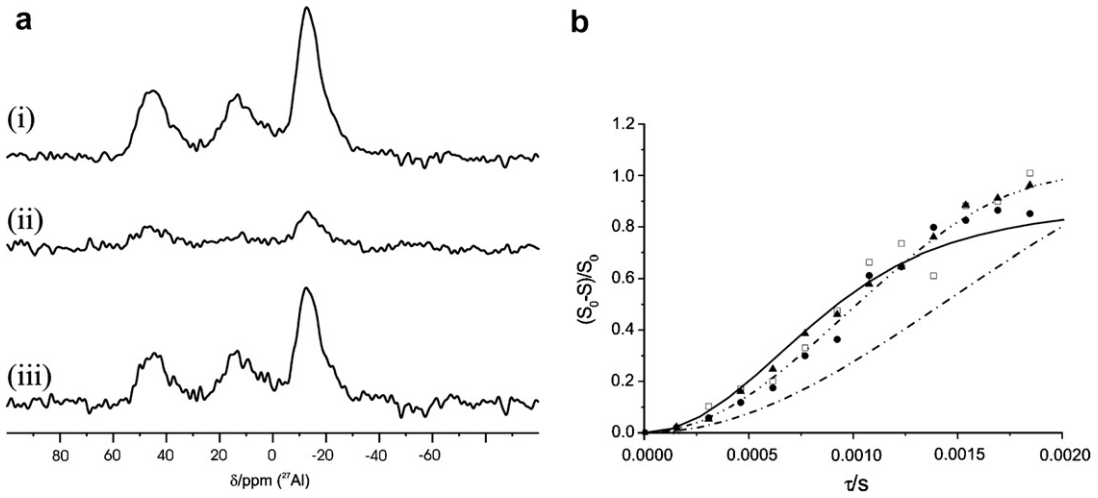

Fig. 8. (a) $^{27}Al\{^{31}P\}$-REDOR NMR spectra for glass KAlP_5 ($\tau = 1.4$ ms). The top spectrum (i) represents the full ^{27}Al echo signal defining S_0 for the individual signals; spectrum (ii) the $^{27}Al\{^{31}P\}$-REDOR-NMR spectrum giving the reduced signal intensities S for the individual signals and (iii) constitutes the difference (i)–(ii); (b) REDOR evolution curves for the individual signals for AlO_4-(full circles), AlO_5-(open squares) and AlO_6-units (full triangles) together with the results of SIMPSON simulations assuming P–Al_x multiple spin interactions (dash–dotted line: AlP_2; dash–dotted–dotted line: AlP_4; solid line: AlP_6).

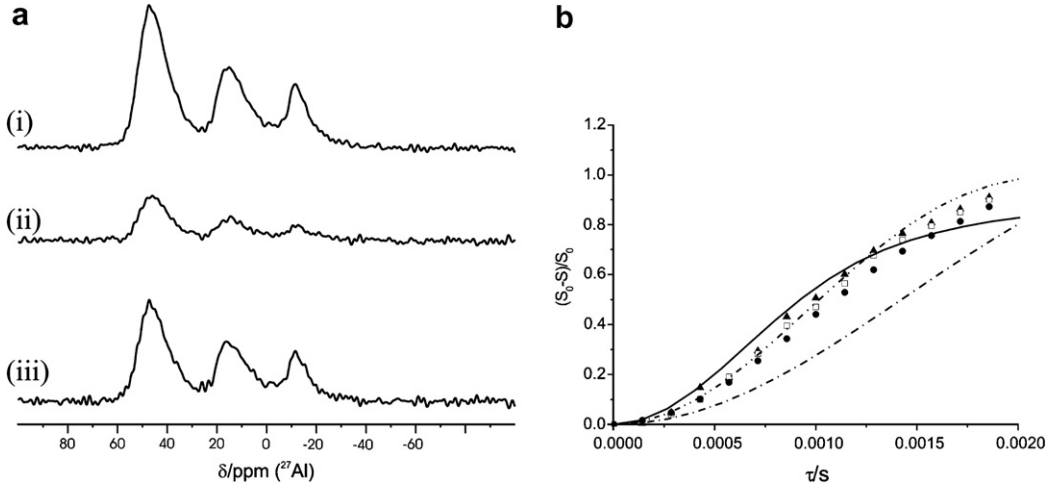

Fig. 9. (a) $^{27}Al\{^{31}P\}$-REDOR NMR spectra for glass KAlP_12.5 ($\tau = 1.4$ ms). The arrangement of the spectra resembles that of Fig. 8(a). (b) REDOR evolution curves for the individual signals for AlO_4-(full circles), AlO_5-(open squares) and AlO_6-units (full triangles) together with the results of SIMPSON simulations assuming P–Al_x multiple spin interactions (dash–dotted line: AlP_2; dash–dotted–dotted line: AlP_4; solid line: AlP_6).

the relative fractions of the different Q^n_{m,AlO_x} units (cf. Table 3) and AlO_x species we can further characterize the local AlO_x environment: AlO_6 is connected to two Q^1_2 and four Q^1_1 species, whereas AlO_4 is connected to four Q^1_1 moieties. The main local phosphate structural motifs as found in the low alumina glasses are depicted in Fig. 10(a), an extended network fragment incorporating the $^{27}Al\{^{31}P\}$-REDOR NMR results is sketched in Fig. 10(b). The compliance of the observed phosphate and aluminate site speciation with the composition can be checked as follows. Assuming the applicability of Loewenstein's rule as indicated by the $^{27}Al\{^{31}P\}$-REDOR NMR results we need 53 phosphate polyhedra to fully coordinate the 10 aluminate polyhedra (2.5 AlO_4, 2.0 AlO_5 and 5.5 AlO_6, cf. Table 2). This value proves to be in reasonable agreement with the result from a site speciation for the phosphate species (cf. Table 3) which produces 9 Q^1_{1,AlO_4} 26 Q^1_{1,AlO_6} and 11 Q^1_{2,AlO_6} giving *in toto* 57 phosphate tetrahedra to fully saturate the 10 aluminate polyhedra.

Medium Al_2O_3 content glasses: Up to an alumina content of 10%, the glass structure is built from the same phosphate and aluminate moieties as described before. The decrease of the fraction of hexa-coordinated aluminium with increasing alumina content is accompanied by a concomitant decrease in the fraction of Q^1_{n,AlO_6} ($n = 1, 2$) with the latter disappearing for alumina contents $> 10\%$. At the same time, the fractions of Q^1_{1,AlO_5} and Q^1_{1,AlO_4} are increasing. For KAlP_10, 60 phosphate tetrahedra are needed to fully coordinate the penta- and hexa-coordinated aluminium and 36 phosphate units to coordinate the AlO_4

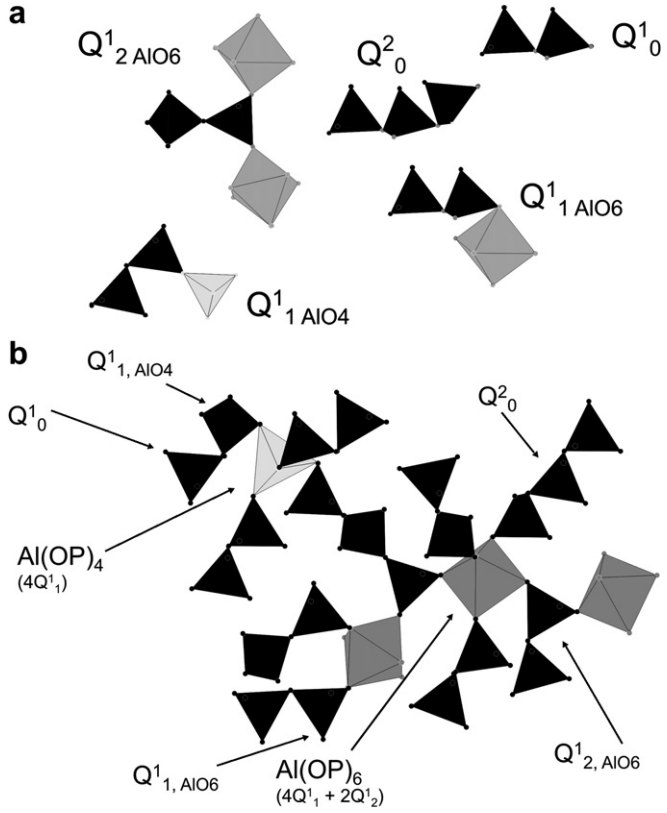

Fig. 10. (a) Main Q^n_m structural motifs dominating the network for low-alumina glasses; (b) sketch of an extended network fragment.

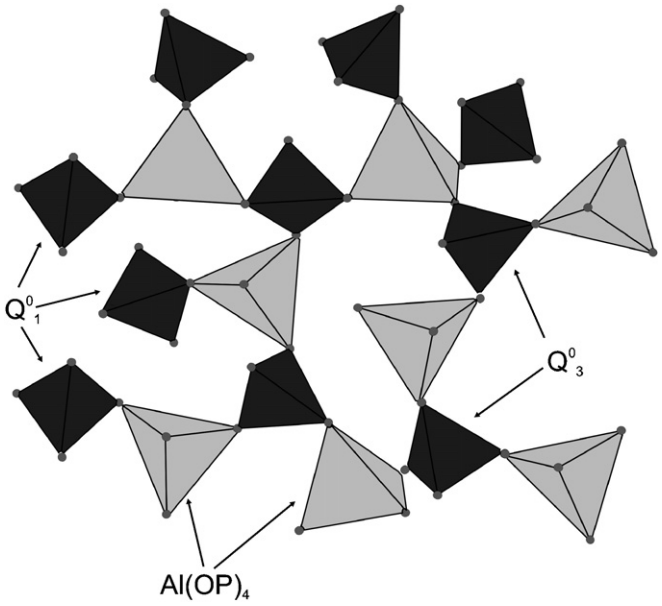

Fig. 11. Network organization for the high alumina glasses exhibiting Q^0_{3,AlO_4} and $Al(OP)_4$ as the dominating structural motifs on intermediate length scales.

groups. The site speciation for the phosphate groups produced 53 phosphate polyhedra for the coordination of the AlO_5 and AlO_6 groups and 28 phosphate polyhedra for the tetra-coordinated aluminate species. The somewhat low number for the phosphate groups for the coordination of the AlO_4 groups might be explained by the presence of a (low) amount of Q^0_{3,AlO_4} units which could not be deconvoluted from the Q^1_{1,AlO_4} and Q^1_{1,AlO_6} species.

High Al_2O_3 content glasses: In these glasses AlO_4 units constitute the dominating aluminium polyhedra and the high alumina content imparts a further depolymerisation of the phosphate network. $Q^1_{1,AlO_{5/6}}$ and $Q^1_{2,AlO_{5/6}}$ as the main phosphate species dominating at low and intermediate alumina content are successively replaced by two new species at +3 ppm and −6 ppm, which could be identified (in the KAlP_20 sample) as a Q^0_{1,AlO_4} (+3.5 ppm) species, formed by the reaction between a Q^1_0 and aluminium ($Q^1_0 + AlO_4 \rightarrow Q^0_{1,AlO_4}$) and a Q^0_{3,AlO_4} species (−6 ppm), formed via $Q^1_2 + AlO_4 \rightarrow Q^0_{3,AlO_4}$. In Fig. 11, an extended fragment of the network organization in the high alumina glasses is sketched. The depolymerisation has continued to produce very short phosphate chains and the identified Q^0_m, AlO_4 moieties ($m = 1$, 3) together with $Al(OP)_4$ constitute the dominating structural motifs on intermediate length scales. For KAlP_20, 164 P–O–Al bonds are needed to fully coordinate the 38 AlO_4 and 2 AlO_6 polyhedra. From the observed phosphate speciation (i.e., 78% Q^0_{3,AlO_4} and 22% Q^0_{1,AlO_4}) we calculate a total number of 153 P–O–Al-linkages in good agreement with the above, corroborating the network organization as suggested for the high alumina glasses.

5. Conclusion

We presented a study of the network organization in aluminophosphate glasses of general composition $50K_2O$–xAl_2O_3–$(50-x)P_2O_5$ with $0 < x < 20\%$. The evolution of the glass structure upon alumina incorporation into the phosphate network was monitored employing a combination of advanced solid state NMR strategies including $^{31}P\{^{27}Al\}$-CP-HETCOR NMR, $^{31}P\{^{27}Al\}$-REAPDOR NMR, $^{27}Al\{^{31}P\}$-REDOR NMR and 2D ^{31}P-J-RESolved NMR spectroscopy. Aluminum enters the network as AlO_4, AlO_5 and AlO_6 polyhedra which proved to be fully connected to phosphate units, in fulfilment of the Loewenstein rule. The structural motifs on intermediate length scales could be characterized employing a modified Q notation, Q^n_{m,AlO_x}, with n denoting the number of connected phosphate polyhedra, n characterizing the number of connected aluminate polyhedra and x identifying the coordination state of the connected aluminate polyhedra.

The depolymerisation of the phosphate network is evolving from Q^2_0 units which are successively replaced by a set of different Q^1_m moieties connected to either one ($m = 1$) or two ($m = 2$) aluminate units. With increasing alumina content the fraction of Q^2_0 and the Q^1 units connected to penta- and hexa-coordinated aluminium, Q^1_{1,AlO_6} and Q^1_{2,AlO_6} is gradually decreasing and replaced by Q^1_{1,AlO_4} as the dominating phosphate species at intermediate alumina content and finally by Q^0_{1,AlO_4} and Q^0_{3,AlO_4} species at

high alumina content. The incorporation of alumina in excess of 20% proves to be impossible employing standard glass-making procedures.The expected further depolymerisation of the phosphate network for such glasses with the formation of Q^0_{4,AlO_4} phosphate species might however be possible when resorting to sol–gel techniques for the glass preparation.

References

[1] J. Vogel, W. Holand, K. Naumann, J. Gummel, J. Non-Cryst. Solids 80 (1986) 34.
[2] J.A. Wilder, J. Non-Cryst. Solids 38&39 (1980) 879.
[3] I.W. Donald, B.L. Metcalfe, J. Non-Cryst. Solids 348 (2004) 118.
[4] N.J. Kreidl, W.A. Weyl, J. Am. Ceram. Soc. 24 (11) (1941) 372.
[5] R.K. Brow, J. Am. Ceram. Soc. 76 (4) (1993) 913.
[6] R.K. Brow, R.J. Kirkpatrick, G.L. Turner, J. Am. Ceram. Soc. 76 (4) (1993) 919.
[7] A. Belkébir, J. Rocha, A.P. Esculcas, P. Berthet, B. Gilbert, Z. Gabelica, G. Llabres, F. Wijzen, A. Rulmont, Spectrochim. Acta A 55 (1999) 1323.
[8] J.M. Egan, R.M. Wenslow, K.T. Mueller, J. Non-Cryst. Solids 261 (2000) 115.
[9] D.P. Lang, T.M. Alam, D.N. Bencoe, Chem. Mater. 13 (2001) 420.
[10] L. Zhang, H. Eckert, J. Phys. Chem. B 110 (2006) 8946.
[11] S. Wegner, G. Tricot, L. Van Wüllen, Solid State Nucl. Magn. Reson. 32 (2007) 44.
[12] P. Caravatti, G. Bodenhausen, R. Ernst, Chem. Phys. Lett. 89 (5) (1982) 363.
[13] A.J. Vega, Solid State Nucl. Magn. Reson. 1 (1996) 17.
[14] T. Gullion, Chem. Phys. Lett. 246 (1995) 325.
[15] S.P. Brow, M. Pérez-Torralba, D. Sanz, R.M. Claramunt, L. Emsley, Chem. Commun. (2002) 1852.
[16] F. Fayon, I.J. King, R.K. Harris, J.S.O. Evans, D. Massiot, C.R. Chimie 7 (2004) 351.
[17] T. Gullion, J. Schaefer, J. Magn. Reson. 81 (1989) 196.
[18] S.R. Hartmann, E.L. Hahn, Phys. Rev. 128 (1962) 2042.
[19] M. Bak, J.T. Rasmussen, N.C. Nielsen, J. Magn. Reson. 147 (2000) 296.
[20] E. Metwalli, R.K. Brow, J. Non-Cryst. Solids 289 (2001) 113.
[21] Y.B. Peng, D.E. Day, Glass Technol. 32 (5) (1991) 166.
[22] G. Tricot, L. Montagne, L. Delevoye, G. Palavit, V. Kostoj, J. Non-Cryst. Solids 345&346 (2004) 56.
[23] H.N. Ng, C. Calvo, Can. J. Chem. 51 (16) (1973) 2613.
[24] R.N. Devi, K. Vidyasagar, Inorg. Chem. 39 (2000) 2391.
[25] A.R. Grimmer, U. Haubenreisser, Chem. Phys. Lett. 99 (1983) 487.
[26] D. Massiot, F. Fayon, M. Capron, I. King, S. Le Calvé, B. Alonso, J-O. Durand, B. Bujoli, Z. Gan, G. Hoatson, Magn. Res. Chem. 40 (2002) 70.
[27] W. Löwenstein, Am. Miner. 39 (1954) 92.
[28] J.C.C. Chan, H. Eckert, J. Magn. Reson. 147 (2000) 170.
[29] M. Feike, D.E. Demco, R. Graf, J. Gottwald, S. Hafner, H.W. Spiess, J. Magn. Reson. A 122 (1996) 214.
[30] A. Bax, R. Freeman, S.P. Kempbell, J. Am. Chem. Soc. 102 (1980) 4849.